

THEORETICAL AND NUMERICAL ASPECTS IN
WEAK-COMPRESSIBLE FINITE STRAIN
THERMO-ELASTICITY

AHMAD-WAHADJ HAMKAR
STEFAN HARTMANN

*Clausthal University of Technology, Institute of Applied Mechanics, Clausthal-Zellerfeld, Germany
e-mail: stefan.hartmann@tu-clausthal.de*

In this essay, a constitutive model for nearly incompressible elastic behavior is extended to the case to thermal effects. First, the use is made of the multiplicative decomposition of the deformation gradient into a thermal and a mechanical part. The thermal part is purely volumetric. Additionally, the mechanical part is multiplicatively decomposed into a volume-preserving and a volume-changing part so that the final stress state shows the influences of the temperature-dependence. The proposed model is carefully studied in view of the thermo-mechanical coupling effects. Second, the model is implemented into a time-adaptive finite element formulation based on higher-order Rosenbrock-type methods, which is a completely iteration-free procedure so that really fast computations are available. The article concludes with a three-dimensional numerical simulation of a representative elastomeric tensile specimen.

Key words: thermoelasticity, finite strains, finite elements, Rosenbrock-type methods

1. Introduction

The incorporation of thermo-mechanical coupling effects starts with the decomposition of the deformation gradient $\mathbf{F}(\vec{X}, t) = \text{Grad } \vec{\chi}_R(\vec{X}, t)$, into a thermal and a mechanical part $\mathbf{F} = \mathbf{F}_M \mathbf{F}_\Theta$, where $\vec{x} = \vec{\chi}_R(\vec{X}, t)$ defines motion of a particle \vec{X} occupying the place \vec{x} at time t . This proposal of Lu and Pister (1975) is taken up in a number of papers (see Miehe, 1988; Holzapfel and Simo, 1996b; Lion, 1997; Heimes, 2005). An additional decomposition of the mechanical part into a volume-changing and volume-preserving part goes

back to Flory (1961). There, a particular assumption of the free-energy yields a clear assignment of kinematical quantities to the hydrostatic and deviatoric Cauchy stress state. Since the thermal deformation is purely volumetric, this approach is of particular interest for thermo-mechanical deformation processes as well. References with similar approaches are given by Simo and Miehe (1992), Miehe (1995), Holzapfel and Simo (1996a).

In the case of isothermal problems, it was found out that for Rivlin-Saunders type models, see for a detailed investigation in Hartmann (2001a,b), it is not possible to show the existence of a solution if the models are extended to the case of nearly incompressibility (see Hartmann and Neff, 2003). Accordingly, Hartmann and Neff (2003) proposed a new class of strain-energy functions, which are based on invariants of the unimodular right or left Cauchy-Green tensors. One additional aspect lies in the fact that nearly all hyperelasticity relations, which are based on the decomposition into volume-preserving and volume-changing parts, show non-physical behavior in the tensile and compression test, see Ehlers and Eipper (1998) as well. However, in Hartmann and Neff (2003) it is shown that this essentially depends on the choice of the parts in the free-energy. Since thermo-mechanical coupled problems essentially depend on the volume-change, at least resulting from the volumetric temperature expansion, the investigations have to be extended to thermoelasticity, which is done in this paper.

In contrast to Miehe (1995) and Holzapfel and Simo (1996a) other functions of the free-energy function are applied, and the derivation of the heat equation is based here on the proposed decomposition of the deformation gradient. The latter leads to a consistent representation leading to an exact expression of the thermo-elastic coupling term and the specific heat capacity. This strict derivative has only been carried out by Lion (1997) for the case of incompressibility and without any scopes for the numerical treatment, which results in a different formulation.

A second important aspect treats the implementation of the constitutive model into a finite element program. Commercial programs have the difficulty that the heat equation does not offer the possibility to incorporate an arbitrary process-dependent heat source so that a real thermo-mechanical coupled problem is not able to be computed. Moreover, staggered schemes, which have their advantages in the application of two independent codes (a pure thermal and a pure mechanical one), cannot guarantee to follow the exact solution. Moreover, these are time-integration methods of the order one. Accordingly, an efficient fully monolithic finite element approach has to be developed. In this context, we pick up a very efficient finite element concept developed in

Hartmann and Wensch (2007), Hartmann and Hamkar (2010) for the case of isothermal problems. Due to the fact that both the discretized heat equation in the finite element framework represents a system of ordinary differential equations and the discretized weak formulation of the equilibrium conditions (or principle of virtual displacements), which define a system of non-linear equations, are coupled, Rosenbrock-type methods are applied to the resulting system of differential-algebraic equations (DAE-system). This is done in this work for the first time. Because of the superior behavior of Rosenbrock-type methods on the case of smooth problems, which lead after the time-discretization of the DAE-system only to the solution of a linear system of equations within each point in time (see Hartmann and Wensch, 2007; Hartmann and Hamkar, 2010; Lang, 2000) in the context of finite elements, very efficient and consistent computations are obtained. Moreover, the use is made of higher-order time-integration methods and a time-adaptive procedure (step-size control).

The paper is organized as follows: first, the thermo-mechanically coupled constitutive model is developed. Afterwards, the resulting DAE-system is derived showing the coupling aspects. Finally, a numerical example using the fully iteration-free method for a problem with different time-scales is considered. The notation in use is defined in the following manner: geometrical vectors are symbolized by \vec{a} , second order tensors \mathbf{A} by bold-faced Roman letters, and calligraphic letters \mathcal{A} define fourth order tensors. Furthermore, we introduce matrices at the global level symbolized by bold-faced italic letters \mathbf{A} .

2. Constitutive assumptions

In order to develop the constitutive model, the multiplicative decomposition of the deformation gradient \mathbf{F} into a thermal \mathbf{F}_Θ and a mechanical part \mathbf{F}_M according to the proposal of Lu and Pister (1975) is assumed

$$\mathbf{F} = \mathbf{F}_\Theta \mathbf{F}_M \quad (2.1)$$

Additionally, the mechanical part

$$\mathbf{F}_M = \hat{\mathbf{F}}_M \bar{\mathbf{F}}_M \quad (2.2)$$

is decomposed into a volume-preserving part $\bar{\mathbf{F}}_M$ and a volume-changing part $\hat{\mathbf{F}}_M$ according to Flory (1961)

$$\begin{aligned} \hat{\mathbf{F}}_M &= (\det \mathbf{F}_M)^{1/3} \mathbf{I} & \det \hat{\mathbf{F}}_M &= \det \mathbf{F}_M \\ \bar{\mathbf{F}}_M &= (\det \mathbf{F}_M)^{-1/3} \mathbf{F}_M & \det \bar{\mathbf{F}}_M &= 1 \end{aligned} \quad (2.3)$$

The thermal part is assumed to be purely volumetric

$$\mathbf{F}_\Theta = \varphi^{1/3} \mathbf{I} \quad \varphi = \hat{\varphi}(\Theta - \Theta_0) = \hat{\varphi}(\vartheta) \quad (2.4)$$

where $\hat{\varphi}(0) = 1$ should hold and the temperature difference $\vartheta = \Theta - \Theta_0$ is defined. Θ is the absolute temperature and Θ_0 defines the reference temperature. The determinant of the thermal deformation is obviously given by

$$\det \mathbf{F}_\Theta = \hat{\varphi}(\Theta - \Theta_0) = \hat{\varphi}(\vartheta) \quad (2.5)$$

describing the volumetric deformation caused by the temperature change ϑ , which is chosen to be linear in view of observations in elastomers

$$\hat{\varphi}(\Theta - \Theta_0) := 1 + \alpha(\Theta - \Theta_0) = 1 + \alpha\vartheta \quad (2.6)$$

see Treloar (1975). In view of the total deformation

$$\det \mathbf{F} = \det(\mathbf{F}_\Theta \mathbf{F}_M) = (\det \mathbf{F}_\Theta)(\det \mathbf{F}_M) = \hat{\varphi}(\Theta - \Theta_0)(\det \mathbf{F}_M) \quad (2.7)$$

holds. Accordingly, we have

$$\mathbf{F} = \hat{\mathbf{F}} \bar{\mathbf{F}} \quad \text{with} \quad \begin{cases} \hat{\mathbf{F}} &= (\varphi \det \mathbf{F}_M)^{1/3} \mathbf{I} \\ \bar{\mathbf{F}} &= \bar{\mathbf{F}}_M \end{cases} \quad (2.8)$$

with $\bar{\mathbf{F}} = (\det \mathbf{F})^{-1/3} \mathbf{F}$. Sometimes it is useful to introduce the abbreviation for the determinants $J := \det \mathbf{F} = J_\Theta J_M$, $J_\Theta := \det \mathbf{F}_\Theta = \varphi$ and $J_M := \det \mathbf{F}_M = J/\varphi$ which are used later for short notational purposes.

Using the imagination of a fictitious thermal unloading, similar to the case of the multiplicative decomposition of the deformation gradient into an elastic and a plastic state (see Haupt, 1985), the mechanical Green strain tensor

$$\mathbf{E}_M := \lim_{\vartheta \rightarrow 0} \mathbf{E} = \frac{1}{2}(\mathbf{F}_M^\top \mathbf{F}_M - \mathbf{I}) \quad (2.9)$$

is defined, where

$$\mathbf{E} = \frac{1}{2}(\mathbf{F}^\top \mathbf{F} - \mathbf{I}) \quad (2.10)$$

is the Green strain tensor itself. This motivates the thermal part of the Green-Lagrange-type

$$\mathbf{E}_\Theta = \mathbf{E} - \mathbf{E}_M = \frac{1}{2}(\mathbf{F}^\top \mathbf{F} - \mathbf{F}_M^\top \mathbf{F}_M) = \frac{1}{2}(\mathbf{C} - \mathbf{C}_M) \quad (2.11)$$

or vice versa the additive decomposition

$$\mathbf{E} = \mathbf{E}_M + \mathbf{E}_\Theta \quad (2.12)$$

The push-forward operation $\mathbf{F}_M^{-\top} \mathbf{E} \mathbf{F}_M^{-1}$ yields the decomposition

$$\hat{\mathbf{\Gamma}} = \hat{\mathbf{\Gamma}}_M + \hat{\mathbf{\Gamma}}_\Theta \quad (2.13)$$

with

$$\begin{aligned} \hat{\mathbf{\Gamma}} &= \mathbf{F}_M^{-\top} \mathbf{E} \mathbf{F}_M^{-1} = \frac{1}{2}(\mathbf{F}_\Theta^\top \mathbf{F}_\Theta - \mathbf{F}_M^{-\top} \mathbf{F}_M^{-1}) = \frac{1}{2}(\varphi^{2/3} \mathbf{I} - \mathbf{B}_M^{-1}) = \frac{\varphi^{2/3}}{3}(\mathbf{I} - \mathbf{B}^{-1}) \\ \hat{\mathbf{\Gamma}}_M &= \mathbf{F}_M^{-\top} \mathbf{E}_M \mathbf{F}_M^{-1} = \frac{1}{2}(\mathbf{I} - \mathbf{F}_M^{-\top} \mathbf{F}_M^{-1}) = \frac{1}{2}(\mathbf{I} - \mathbf{B}_M^{-1}) \\ \hat{\mathbf{\Gamma}}_\Theta &= \mathbf{F}_M^{-\top} \mathbf{E}_\Theta \mathbf{F}_M^{-1} = \frac{1}{2}(\mathbf{F}_\Theta^\top \mathbf{F}_\Theta - \mathbf{I}) = \frac{1}{2}(\mathbf{C}_\Theta - \mathbf{I}) = \frac{1}{2}(\varphi^{2/3} - 1)\mathbf{I} \end{aligned} \quad (2.14)$$

where $\hat{\mathbf{\Gamma}}$, $\hat{\mathbf{\Gamma}}_M$ and $\hat{\mathbf{\Gamma}}_\Theta$ measure the strains relative to the mechanical intermediate configuration \mathcal{B}_M . Here, the right and left Cauchy-Green tensors

$$\begin{aligned} \mathbf{C} &= \mathbf{F}^\top \mathbf{F} & \mathbf{C}_\Theta &= \mathbf{F}_\Theta^\top \mathbf{F}_\Theta = \varphi^{2/3} \mathbf{I} & \mathbf{C}_M &= \mathbf{F}_M^\top \mathbf{F}_M = \varphi^{-2/3} \mathbf{C} \\ \mathbf{B} &= \mathbf{F} \mathbf{F}^\top & \mathbf{B}_\Theta &= \mathbf{F}_\Theta \mathbf{F}_\Theta^\top = \varphi^{2/3} \mathbf{I} & \mathbf{B}_M &= \mathbf{F}_M \mathbf{F}_M^\top = \varphi^{-2/3} \mathbf{B} \end{aligned} \quad (2.15)$$

are introduced. The definition of strain measures (2.14)_{2,3} have the advantage that they are purely mechanical and purely thermal. For later purposes, the mechanical deformation is decomposed into volume-changing and preserving parts, defined by $J_M = \det \mathbf{F}_M = (\det \mathbf{C}_M)^{1/2}$ and the unimodular, mechanical right Cauchy-Green tensor $\overline{\mathbf{C}}_M = (\det \mathbf{C}_M)^{-1/3} \mathbf{C}_M$, $\det \overline{\mathbf{C}}_M = 1$, is introduced.

Additionally, strain-rate tensors relative to the mechanical intermediate configuration \mathcal{B}_M can be defined on the basis of the material time derivative of (2.9)-(2.11) by the corresponding push-forward operation $\mathbf{F}_M^{-\top} (\dot{\mathbf{E}}) \mathbf{F}_M^{-1}$. This yields the strain-rate measures relative to the intermediate configuration \mathcal{B}_M

$$\begin{aligned} \overset{\Delta}{\hat{\mathbf{\Gamma}}} &= \mathbf{F}_M^{-\top} \dot{\mathbf{E}} \mathbf{F}_M^{-1} = \dot{\hat{\mathbf{\Gamma}}} + \mathbf{L}_M^\top \hat{\mathbf{\Gamma}} + \hat{\mathbf{\Gamma}} \mathbf{L}_M \\ \overset{\Delta}{\hat{\mathbf{\Gamma}}_M} &= \mathbf{F}_M^{-\top} \dot{\mathbf{E}}_M \mathbf{F}_M^{-1} = \dot{\hat{\mathbf{\Gamma}}_M} + \mathbf{L}_M^\top \hat{\mathbf{\Gamma}}_M + \hat{\mathbf{\Gamma}}_M \mathbf{L}_M = \frac{1}{2}(\mathbf{L}_M + \mathbf{L}_M^\top) =: \mathbf{D}_M \\ \overset{\Delta}{\hat{\mathbf{\Gamma}}_\Theta} &= \mathbf{F}_M^{-\top} \dot{\mathbf{E}}_\Theta \mathbf{F}_M^{-1} = \dot{\hat{\mathbf{\Gamma}}_\Theta} + \mathbf{L}_M^\top \hat{\mathbf{\Gamma}}_\Theta + \hat{\mathbf{\Gamma}}_\Theta \mathbf{L}_M \end{aligned} \quad (2.16)$$

and implies the additive decomposition

$$\hat{\mathbf{\Gamma}} \stackrel{\Delta}{=} \hat{\mathbf{\Gamma}}_M + \hat{\mathbf{\Gamma}}_\Theta \quad (2.17)$$

The strain-rate $\hat{\mathbf{\Gamma}}_M$ is purely mechanical, whereas the thermal strain-rate relative to the intermediate state can be calculated by

$$\hat{\mathbf{\Gamma}}_\Theta = \underbrace{\frac{1}{3}\dot{\varphi}'(\Theta - \Theta_0)\dot{\Theta}(t)\varphi^{-1/3}\mathbf{I}}_{\dot{\mathbf{r}}_\Theta} + (\varphi^{2/3} - 1)\hat{\mathbf{\Gamma}}_M \quad (2.18)$$

see Eqs. (2.16)₃, (2.14)₃, and (2.16)₂.

Next, these strain measures are used within the specific stress power to develop appropriate stress measures according to the concept of dual variables (Haupt and Tsakmakis, 1989, 1996)

$$p = \frac{1}{\rho}\mathbf{T} \cdot \mathbf{D} = \frac{1}{\rho_R}\tilde{\mathbf{T}} \cdot \dot{\mathbf{E}} = \frac{1}{\rho_R}\tilde{\mathbf{T}} \cdot (\mathbf{F}_M^\top \hat{\mathbf{\Gamma}} \mathbf{F}_M) = \frac{1}{\rho_R}(\mathbf{F}_M \tilde{\mathbf{T}} \mathbf{F}_M^\top) \cdot \hat{\mathbf{\Gamma}} = \frac{1}{\rho_R}\hat{\mathbf{S}}_M \cdot \hat{\mathbf{\Gamma}} \quad (2.19)$$

Here, Eq. (2.16)₁ is exploited and a Kirchhoff-type stress tensor relative to the mechanical intermediate configuration

$$\hat{\mathbf{S}}_M = \mathbf{F}_M \tilde{\mathbf{T}} \mathbf{F}_M^\top \quad (2.20)$$

is introduced. $\tilde{\mathbf{T}} = (\det \mathbf{F})\mathbf{F}^{-1}\mathbf{T}\mathbf{F}^{-\top}$ defines the second Piola-Kirchhoff stress tensor, \mathbf{T} the Cauchy stress tensor and $\mathbf{D} = (\mathbf{L} + \mathbf{L}^\top)/2$ the spatial strain-rate tensor depending on the spatial velocity gradient $\mathbf{L} = \dot{\mathbf{F}}\mathbf{F}^{-1}$. Inserting strain-rates (2.17) and (2.18) into specific stress power (2.19), leads to

$$\begin{aligned} p &= \frac{1}{\rho_R}\hat{\mathbf{S}}_M \cdot \hat{\mathbf{\Gamma}} = \frac{1}{\rho_R}\hat{\mathbf{S}}_M \cdot (\hat{\mathbf{\Gamma}}_M + \hat{\mathbf{\Gamma}}_\Theta) \\ &= \frac{1}{\rho_R}\varphi^{2/3}\hat{\mathbf{S}}_M \cdot \hat{\mathbf{\Gamma}}_M + \frac{\dot{\varphi}'(\Theta - \Theta_0)\varphi^{-1/3}\dot{\Theta}(t)}{3\rho_R}(\text{tr } \hat{\mathbf{S}}_M) \end{aligned} \quad (2.21)$$

In view of thermo-mechanical processes, the Clausius-Duhem inequality has to be fulfilled

$$-\dot{\psi} - \dot{\Theta}s + \frac{1}{\rho_R}\tilde{\mathbf{T}} \cdot \dot{\mathbf{E}} - \frac{\vec{q}}{\rho\Theta} \cdot \text{grad } \Theta = -\dot{\psi} - \dot{\Theta}s + \frac{1}{\rho_R}\mathbf{S}_M \cdot \hat{\mathbf{\Gamma}} - \frac{\vec{q}}{\rho\Theta} \cdot \text{grad } \Theta \geq 0 \quad (2.22)$$

where ψ defines the specific free-energy, s is the entropy, and \vec{q} the heat flux vector. In the following, the proposals of Lion (2000) and Heimes (2005) are taken up implying the assumption that the free-energy depends on the mechanical deformation \mathbf{E}_M and the temperature Θ

$$\psi(\mathbf{E}_M, \Theta) = \psi_M(\mathbf{C}_M, \Theta) + \psi_\Theta(\Theta) \quad (2.23)$$

The mechanical part is assumed to be linear in the temperature

$$\psi_M(\mathbf{C}_M, \Theta) = \frac{\Theta}{\Theta_0} \bar{\psi}_M(\mathbf{C}_M) \quad (2.24)$$

with

$$\bar{\psi}_M(\mathbf{C}_M) = U(J_M) + \bar{v}(\bar{\mathbf{C}}_M) = U(J_M) + w(\mathbf{I}_{\bar{\mathbf{C}}_M}, \mathbf{II}_{\bar{\mathbf{C}}_M}) \quad (2.25)$$

which is decomposed into a free-energy $U(J_M)$ depending on the purely volumetric, mechanical deformation and a part depending on the isochoric mechanical deformation. In the later examples, the use is made of

$$\begin{aligned} U(J_M) &= \frac{K}{50}(J_M^5 + J_M^{-5} - 2) \\ w(\mathbf{I}_{\bar{\mathbf{B}}}, \mathbf{II}_{\bar{\mathbf{B}}}) &= \hat{\alpha}(\mathbf{I}_{\bar{\mathbf{B}}}^3 - 27) + c_{10}(\mathbf{I}_{\bar{\mathbf{B}}} - 3) + c_{01}(\mathbf{II}_{\bar{\mathbf{B}}}^{3/2} - 3\sqrt{3}) \end{aligned} \quad (2.26)$$

proposed by Hartmann and Neff (2003) as one possibility in the class of polyconvex strain-energy functions. The thermal part of strain-energy (2.23) is defined by

$$\psi_\Theta(\Theta) = \frac{c_p}{\rho R} \left[\left((\Theta - \Theta_0) - \Theta \ln \frac{\Theta}{\Theta_0} \right) (1 - k_p \Theta_0) - \frac{1}{2} k_p (\Theta^2 - \Theta_0^2) \right] \quad (2.27)$$

resulting from the experimental observation of the linear temperature-dependence of the heat capacity (see Heimes, 2005).

The evaluation of the material time-derivative of the free-energy ψ defined in Eq. (2.23)

$$\dot{\psi}(\mathbf{E}_M, \Theta) = \left(\frac{1}{\Theta_0} \bar{\psi}_M(\mathbf{C}_M) \right) \dot{\Theta} + \frac{\Theta}{\Theta_0} \frac{d\bar{\psi}_M(\mathbf{C}_M)}{d\mathbf{C}_M} \cdot \dot{\mathbf{C}}_M + \psi'_\Theta(\Theta) \dot{\Theta} \quad (2.28)$$

is required in Clausius-Duhem inequality (2.22) yielding, by means of definition (2.20) and the time derivative of (2.9) expressed by mechanical right Cauchy-

Green tensor (2.15)₃, $\dot{\mathbf{C}}_M = 2\mathbf{F}_M^\top \overset{\Delta}{\hat{\mathbf{F}}}_M \mathbf{F}_M$

$$\begin{aligned} & \left(\frac{1}{\rho_R} \varphi^{2/3} \hat{\mathbf{S}}_M - 2 \frac{\Theta}{\Theta_0} \mathbf{F}_M \frac{d\bar{\psi}_M(\mathbf{C}_M)}{d\mathbf{C}_M} \mathbf{F}_M^\top \right) \cdot \overset{\Delta}{\hat{\mathbf{F}}}_M \\ & + \left[-s - \left(\frac{1}{\Theta_0} \bar{\psi}_M(\mathbf{C}_M) + \psi'_\Theta(\Theta) \right) + \frac{1}{3\rho_R} \varphi^{-1/3} \dot{\varphi}'(\Theta - \Theta_0) \text{tr} \hat{\mathbf{S}}_M \right] \dot{\Theta} \\ & - \frac{\vec{q}}{\rho\Theta} \cdot \text{grad } \Theta \geq 0 \end{aligned} \quad (2.29)$$

Exploiting arbitrary mechanical strain and temperature paths, implies the three following expressions

$$\begin{aligned} \hat{\mathbf{S}}_M &= \frac{2\rho_R}{\varphi^{2/3}} \frac{\Theta}{\Theta_0} \mathbf{F}_M \frac{d\bar{\psi}_M(\mathbf{C}_M)}{d\mathbf{C}_M} \mathbf{F}_M^\top \\ s &= -\frac{1}{\Theta_0} \bar{\psi}_M(\mathbf{C}_M) - \psi'_\Theta(\Theta) + \frac{1}{3\rho_R} \varphi^{-1/3} \dot{\varphi}'(\Theta - \Theta_0) \text{tr} \hat{\mathbf{S}}_M \\ \vec{q} &= -\kappa \text{grad } \Theta \quad \kappa \geq 0 \end{aligned} \quad (2.30)$$

Having particular strain-energy function (2.25), yields for the derivatives in elasticity relation (2.30)₁

$$\frac{dU((\det \mathbf{C}_M)^{1/2})}{d\mathbf{C}_M} = \frac{1}{2} J_M U'(J_M) \mathbf{C}_M^{-1} \quad (2.31)$$

and

$$\frac{d\bar{v}(\bar{\mathbf{C}}_M(\mathbf{C}_M))}{d\mathbf{C}_M} = \left[\frac{d\bar{\mathbf{C}}_M}{d\mathbf{C}_M} \right]^\top \frac{d\bar{v}}{d\bar{\mathbf{C}}_M} \quad (2.32)$$

with

$$\left[\frac{d\bar{\mathbf{C}}_M}{d\mathbf{C}_M} \right]^\top = (\det \mathbf{C}_M)^{-1/3} \left[\mathcal{I} - \frac{1}{3} (\mathbf{C}_M^{-1} \otimes \mathbf{C}_M) \right] = J_M^{-2/3} \left[\mathcal{I} - \frac{1}{3} (\bar{\mathbf{C}}_M^{-1} \otimes \bar{\mathbf{C}}_M) \right] \quad (2.33)$$

In this expression, the identity tensor of fourth order

$$\mathcal{I} = [\mathbf{I} \otimes \mathbf{I}]^{T_{23}} = \delta_{ik} \delta_{jl} \vec{e}_i \otimes \vec{e}_j \otimes \vec{e}_k \otimes \vec{e}_l \quad (2.34)$$

is introduced expressed relative to Cartesian coordinates, $\mathcal{I}\mathbf{A} = \mathbf{A}$. Obviously, $\mathbf{C}_M^{-1} \otimes \mathbf{C}_M = \bar{\mathbf{C}}_M^{-1} \otimes \bar{\mathbf{C}}_M$ holds. Caused by the particular dependence on

the invariants of the mechanical unimodular right Cauchy-Green tensors, the application of the chain-rule leads to

$$\frac{d\bar{v}}{d\bar{\mathbf{C}}_M} = \frac{\partial w}{\partial \mathbf{I}_{\bar{\mathbf{C}}_M}} \frac{d\mathbf{I}_{\bar{\mathbf{C}}_M}}{d\bar{\mathbf{C}}_M} + \frac{\partial w}{\partial \mathbf{II}_{\bar{\mathbf{C}}_M}} \frac{d\mathbf{II}_{\bar{\mathbf{C}}_M}}{d\bar{\mathbf{C}}_M} = (w_1 + w_2 \mathbf{I}_{\bar{\mathbf{C}}_M}) \mathbf{I} - w_2 \bar{\mathbf{C}}_M \quad (2.35)$$

with

$$w_1(\mathbf{I}_{\bar{\mathbf{C}}_M}, \mathbf{II}_{\bar{\mathbf{C}}_M}) = \frac{\partial w}{\partial \mathbf{I}_{\bar{\mathbf{C}}_M}} \quad \text{and} \quad w_2(\mathbf{I}_{\bar{\mathbf{C}}_M}, \mathbf{II}_{\bar{\mathbf{C}}_M}) = \frac{\partial w}{\partial \mathbf{II}_{\bar{\mathbf{C}}_M}} \quad (2.36)$$

In other words, we have

$$\begin{aligned} \frac{d\bar{\psi}_M(\mathbf{C}_M)}{d\mathbf{C}_M} &= \frac{J_M}{2} U'(J_M) \mathbf{C}_M^{-1} + 2J_M^{-2/3} \left[\mathcal{I} - \frac{1}{3} \bar{\mathbf{C}}_M^{-1} \otimes \bar{\mathbf{C}}_M \right] \frac{d\bar{v}}{d\bar{\mathbf{C}}_M} \\ &= \frac{J_M^{1/3}}{2} U'(J_M) \bar{\mathbf{C}}_M^{-1} + \frac{2}{J_M^{2/3}} \left((w_1 + w_2 \mathbf{I}_{\bar{\mathbf{C}}_M}) \mathbf{I} \right. \\ &\quad \left. - w_2 \bar{\mathbf{C}}_M - \frac{1}{3} (w_1 \mathbf{I}_{\bar{\mathbf{C}}_M} + 2w_2 \mathbf{II}_{\bar{\mathbf{C}}_M}) \bar{\mathbf{C}}_M^{-1} \right) \end{aligned} \quad (2.37)$$

These expressions are used to express the elasticity relation relative to the current and the reference configuration. First, the push-forward operation of the second Piola-Kirchhoff tensor $\tilde{\mathbf{T}}$ leads to

$$\mathbf{S} = \mathbf{F} \tilde{\mathbf{T}} \mathbf{F}^\top = \mathbf{F} (\mathbf{F}_M^{-1} \mathbf{S}_M \mathbf{F}_M^{-\top}) \mathbf{F}^\top = \mathbf{F}_M \mathbf{F}_\Theta (\mathbf{F}_M^{-1} \mathbf{S}_M \mathbf{F}_M^{-\top}) \mathbf{F}_\Theta^\top \mathbf{F}_M^\top = \varphi^{2/3} \hat{\mathbf{S}}_M \quad (2.38)$$

where the use is made of decomposition (2.1) and Eq. (2.20). $\mathbf{S} = (\det \mathbf{F}) \mathbf{T}$ defines the weighted Cauchy tensor (Kirchhoff stresses). Comparing (2.38) with (2.30)₁, yields

$$\begin{aligned} \mathbf{S} &= 2\rho_R \frac{\Theta}{\Theta_0} \mathbf{F}_M \frac{d\bar{\psi}_M(\mathbf{C}_M)}{d\mathbf{C}_M} \mathbf{F}_M^\top = \rho_R \frac{\Theta}{\Theta_0} J_M U'(J_M) \mathbf{I} \\ &\quad + 2\rho_R \frac{\Theta}{\Theta_0} J_M^{-2/3} [\mathbf{F}_M \otimes \mathbf{F}_M]^{T_{23}} \left[\mathcal{I} - \frac{1}{3} \mathbf{C}_M^{-1} \otimes \mathbf{C}_M \right] \frac{d\bar{v}}{d\bar{\mathbf{C}}_M} \\ &= \rho_R \frac{\Theta}{\Theta_0} J_M U'(J_M) \mathbf{I} + 2\rho_R \frac{\Theta}{\Theta_0} \left(\bar{\mathbf{F}}_M \frac{d\bar{v}}{d\bar{\mathbf{C}}_M} \bar{\mathbf{F}}_M^\top \right)^D \end{aligned} \quad (2.39)$$

$\mathbf{A}^D = \mathbf{A} - \frac{1}{3} (\text{tr } \mathbf{A}) \mathbf{I}$ defines the deviator operator and $\text{tr } \mathbf{A} = a_k^k$ denotes the trace operator of the second-order tensor. Here, the properties $[\mathbf{A} \otimes \mathbf{B}]^{T_{23}} [\mathbf{C} \otimes \mathbf{D}] = [\mathbf{A} \mathbf{C} \mathbf{B}^\top \otimes \mathbf{D}]$ and $[\mathbf{C} \otimes \mathbf{D}] [\mathbf{A} \otimes \mathbf{B}]^{T_{23}} = [\mathbf{C} \otimes \mathbf{A}^\top \mathbf{D} \mathbf{B}]$ for the expression

$$[\mathbf{F}_M \otimes \mathbf{F}_M]^{T_{23}} \left[\mathcal{I} - \frac{1}{3} \mathbf{C}_M^{-1} \otimes \mathbf{C}_M \right] = \left[\mathcal{I} - \frac{1}{3} \mathbf{I} \otimes \mathbf{I} \right] [\mathbf{F}_M \otimes \mathbf{F}_M]^{T_{23}} \quad (2.40)$$

are exploited. $[\cdot]^{T_{23}}$ symbolizes the transposition of the second and third index of the fourth-order tensors, see for further properties (Hartman, 2002, p. 1464). In conclusion, under the assumption of isotropy and the mechanical unimodular left Cauchy-Green tensor

$$\bar{\mathbf{B}}_M = J_M^{-2/3} \mathbf{B}_M = (J/\varphi)^{-2/3} \varphi^{-2/3} \mathbf{B} = J^{-2/3} \mathbf{B} = \bar{\mathbf{B}}, \quad (2.41)$$

the Cauchy stress tensor

$$\mathbf{T} = \frac{\rho_R}{\varphi} \frac{\Theta}{\Theta_0} U'(J/\varphi) \mathbf{I} + \frac{2\rho_R}{J} \frac{\Theta}{\Theta_0} \left(\frac{d\bar{\mathbf{v}}}{d\bar{\mathbf{B}}} \bar{\mathbf{B}} \right)^D \quad (2.42)$$

is obtained. Finally, the entropy (2.30)₂ results in

$$\begin{aligned} s &= -\frac{1}{\Theta_0} \bar{\psi}_M(\mathbf{C}_M) - \psi'_\Theta(\Theta) + \frac{1}{3\rho_R} \varphi^{-1/3} \hat{\varphi}'(\Theta - \Theta_0) \operatorname{tr} \mathbf{S} \\ &= -\frac{1}{\Theta_0} \left(U\left(\frac{J}{\varphi}\right) + \bar{v}(\bar{\mathbf{C}}) \right) - \psi'_\Theta(\Theta) + \frac{\Theta}{\Theta_0} \frac{\hat{\varphi}'(\Theta - \Theta_0)}{\varphi^2} J U'\left(\frac{J}{\varphi}\right) \end{aligned} \quad (2.43)$$

using relation (2.38).

3. Boundary-value problem and discretization

In the following the numerical treatment of the underlying equations are discussed. The heat equation in the spatial representation is given by

$$\dot{e}(\vec{x}, t) = -\frac{1}{\rho(\vec{x}, t)} \operatorname{div} \vec{q}(\vec{x}, t) + r(\vec{x}, t) + p(\vec{x}, t) \quad (3.1)$$

with the specific internal energy e , the density in the current configuration ρ , the heat flux vector \vec{q} , the volume distributed heat source r , which is assumed to be zero in the following, and the stress power p defined in Eq. (2.19) (see Haupt, 2002, p. 124). Frequently, the specific internal energy e is expressed by $e = \psi + \Theta s$ requiring the time-derivative $\dot{e} = \dot{\psi} + \dot{\Theta} s + \Theta \dot{s}$ in heat equation (3.1). Accordingly, the time-derivatives of free-energy (2.23), see Eq. (2.28) as well, and entropy (2.43) are necessary. This leads to the concrete form of the heat equation

$$c_p(\mathbf{C}, \Theta) \dot{\Theta} = \frac{\kappa}{\rho} \operatorname{div} \operatorname{grad} \Theta - \Theta \left(\beta(\mathbf{C}, \Theta) \mathbf{C}^{-1} - \Xi(\mathbf{C}, \Theta) \right) \cdot \dot{\mathbf{C}} \quad (3.2)$$

where Fourier's model for the heat flux $\vec{q} = -\kappa \text{grad } \Theta$ is assumed. In this case, the consistent derivation of the heat capacity reads

$$c_p = J_M \frac{\Theta^2}{\Theta_0} \frac{\hat{\varphi}'}{\varphi} \left[2 \left(\frac{1}{\Theta} + \frac{1}{2} \frac{\hat{\varphi}''}{\hat{\varphi}'} - \frac{\hat{\varphi}'}{\varphi} \right) U'(J_M) - \hat{\varphi}' J_M U''(J_M) \right] - \Theta \psi''_{\Theta}(\Theta) \quad (3.3)$$

Additionally, we have the abbreviations

$$\begin{aligned} \beta(\mathbf{C}, \Theta) &= \frac{1}{2} J_M \frac{\Theta}{\Theta_0} \frac{\hat{\varphi}'}{\varphi} \left[\left(1 - \frac{1}{\Theta} \frac{\hat{\varphi}'}{\varphi} \right) U'(J_M) + J_M U''(J_M) \right] \\ \Xi(\mathbf{C}, \Theta) &= \frac{1}{J^{2/3} \Theta_0} \left[\mathcal{I} - \frac{1}{3} (\mathbf{C}^{-1} \otimes \mathbf{C}) \right] \frac{d\bar{v}}{d\mathbf{C}} \end{aligned} \quad (3.4)$$

Heat equation (3.2) is coupled with the local balance of linear momentum (quasi-static formulation)

$$\text{div } \mathbf{T} + \rho \vec{k} = \vec{0} \quad (3.5)$$

and vice versa, where \vec{k} represents the acceleration of gravity. The spatial discretization of coupled partial differential equations (3.2)-(3.5) using finite elements leads to a system of differential-algebraic equations

$$\begin{aligned} \mathbf{C}_p(t, \mathbf{u}, \Theta) \dot{\Theta} &= \mathbf{r}_{\Theta}(t, \mathbf{u}, \dot{\mathbf{u}}, \Theta) \\ \mathbf{g}(t, \mathbf{u}, \Theta) &= \mathbf{0} \end{aligned} \quad (3.6)$$

where \mathbf{C}_p represents a time-, displacement- and temperature-dependent heat capacity matrix. Here, $\mathbf{u} \in \mathbb{R}^{n_{uu}}$ and $\Theta \in \mathbb{R}^{n_{\Theta u}}$ symbolize the unknown nodal displacements and temperatures, respectively. Three modifications are used to solve the problem: first, we are not only interested in the unknown nodal displacements and temperatures \mathbf{u} and Θ , but also in the nodal reaction forces and the heat fluxes at those nodes where the displacements and temperatures are prescribed. According to Hartmann *et al.* (2008), and the literature cited therein, the method of Lagrange-multipliers is used in order to obtain the reaction forces. The method of Gear (1986), with a similar idea, however, proposed for ODEs, offers the possibility to get the heat fluxes at those nodes, where the temperatures are prescribed. In both cases all nodal displacements and temperatures have to be assumed to be unknown, $\mathbf{u}_a \in \mathbb{R}^{n_{ua}}$ and $\Theta_a \in \mathbb{R}^{n_{\Theta a}}$. Here, $n_{ua} = n_{uu} + n_{up}$, where n_{up} are the number of prescribed nodal displacements and $n_{\Theta p} = n_{\Theta a} - n_{\Theta u}$ defines the number of prescribed nodal temperatures. Accordingly, two constraints have to be considered

$$\begin{aligned} \mathbf{C}_u(t, \mathbf{u}_a(t)) &= \hat{\mathbf{u}} - \bar{\mathbf{u}}(t) = \mathbf{M}_u^{\top} \mathbf{u}_a(t) - \bar{\mathbf{u}}(t) = \mathbf{0} \\ \mathbf{C}_{\Theta}(t, \Theta_a(t)) &= \hat{\Theta} - \bar{\Theta}(t) = \mathbf{M}_{\Theta}^{\top} \Theta_a(t) - \bar{\Theta}(t) = \mathbf{0} \end{aligned} \quad (3.7)$$

The sizes of the vectors are given by $\mathbf{u}_a = \{\mathbf{u}, \hat{\mathbf{u}}\}^\top \in \mathbb{R}^{n_{ua}}$, $\mathbf{u} \in \mathbb{R}^{n_{uu}}$, $\hat{\mathbf{u}} \in \mathbb{R}^{n_{up}}$, $\boldsymbol{\Theta}_a = \{\boldsymbol{\Theta}, \hat{\boldsymbol{\Theta}}\}^\top \in \mathbb{R}^{n_{\Theta a}}$, $\boldsymbol{\Theta} \in \mathbb{R}^{n_{\Theta u}}$, and $\hat{\boldsymbol{\Theta}} \in \mathbb{R}^{n_{\Theta p}}$. $\hat{\mathbf{u}}$ and $\hat{\boldsymbol{\Theta}}$ are those nodal quantities, where the displacements and the temperatures are prescribed by the functions $\bar{\mathbf{u}}(t)$ and $\bar{\boldsymbol{\Theta}}(t)$. The matrices $\mathbf{M}_u^\top = [\mathbf{0}_{n_{up} \times n_{uu}} \mathbf{I}_{n_{up}}]$ and $\mathbf{M}_\Theta^\top = [\mathbf{0}_{n_{\Theta p} \times n_{\Theta u}} \mathbf{I}_{n_{\Theta p}}]$ filter the required information from the total storage information \mathbf{u}_a and $\boldsymbol{\Theta}_a$.

The second aspect treats the problem that in Eq. (3.4) the heat capacity matrix \mathbf{C}_p is a solution-dependent matrix which might become singular in certain applications. For this problem, the proposal of Lubich and Roche (1990) is followed, where the substitution $\dot{\mathbf{u}}_a = \mathbf{D}_u$ and $\dot{\boldsymbol{\Theta}}_a = \mathbf{D}_\Theta$ is introduced.

Finally, it is well-known that the principle of virtual displacements to solve Eq. (3.6)₂ is not appropriate because of volumetric locking effects. Thus, a three-field mixed formulation proposed in Simo *et al.* (1985) or Simo and Taylor (1991) (see Hartmann, 2002; Hartmann and Hamkar, 2010) as well, is applied. To solve the resulting DAE-system

$$\mathbf{F}(t, \mathbf{y}(t), \dot{\mathbf{y}}(t)) := \left\{ \begin{array}{c} \dot{\mathbf{u}}_a - \mathbf{D}_u \\ \dot{\boldsymbol{\Theta}}_a - \mathbf{D}_\Theta \\ \mathbf{g}_a(t, \mathbf{u}_a, \boldsymbol{\Theta}_a) + \mathbf{M}_u \lambda_u \\ \mathbf{C}_p(\boldsymbol{\Theta}_a, \mathbf{u}_a) \mathbf{D}_\Theta - \mathbf{r}_\Theta(t, \mathbf{u}_a, \mathbf{D}_u, \boldsymbol{\Theta}_a) - \mathbf{M}_\Theta \lambda_\Theta \\ \mathbf{C}_u(t, \mathbf{u}_a) \\ \mathbf{C}_\Theta(t, \boldsymbol{\Theta}_a) \end{array} \right\} = \mathbf{0} \quad (3.8)$$

the use is made of a totally iteration-free time-integration method, the so-called Rosenbrock-type method. It has been successfully studied in the context of isothermal problems in Hartmann and Wensch (2007) and Hartmann and Hamkar (2010). The scheme offers the possibility to apply high-order time-integration methods and a step-size control technique (see Hairer and Wanner, 1996). In each point in time (stage) only a system of linear equations has to be solved. The classical method, either fully coupled or staggered, require iterations to solve the entire system. The proposed procedure is embedded in a 3D-finite element program TASA-FEM, where additional aspects for exploiting linear relations of DAE-system (3.8) a priori considered so that the resulting systems of linear equations have merely the size $n_{ua} + n_{\Theta a}$.

4. Examples

Two examples are studied. First, the aspect of physical relevance in the one-dimensional tensile and compression case if applying the standard volumetric

part $U(J_M)$ is discussed. Second, the three-dimensional finite element simulation of an elastomeric specimen using a step-size controlled higher-order Rosenbrock-type method to solve the fully thermo-mechanical coupled problem is shown.

4.1. Uniaxial tensile-compression test for constant temperatures

In the first investigation, the uniaxial tensile and compression test is assumed with constant temperature. In this case, the deformation gradient has the representation $\mathbf{F} = \lambda \vec{e}_1 \otimes \vec{e}_1 + \lambda_Q (\vec{e}_2 \otimes \vec{e}_2 + \vec{e}_3 \otimes \vec{e}_3)$, where λ defines the prescribed axial stretch and λ_Q the unknown lateral stretch in a bar. The determinant of the deformation gradient reads $J = \det \mathbf{F} = \lambda \lambda_Q^2$ and the unimodular left Cauchy-Green tensor of Eq. (2.41) $\overline{\mathbf{B}} = \overline{B} \vec{e}_1 \otimes \vec{e}_1 + \overline{B}_Q (\vec{e}_2 \otimes \vec{e}_2 + \vec{e}_3 \otimes \vec{e}_3)$ with the abbreviations

$$\overline{B} := (\lambda \lambda_Q^2)^{-2/3} \lambda^2 \quad \text{and} \quad \overline{B}_Q := (\lambda \lambda_Q^2)^{-2/3} \lambda_Q^2$$

The stress state is given by $\mathbf{T} = \sigma \vec{e}_1 \otimes \vec{e}_1$, which has to be inserted into thermo-elasticity relation (2.42). This leads with

$$\frac{d\overline{v}}{d\overline{\mathbf{B}}} \overline{\mathbf{B}} = (w_1 + w_2 \mathbf{I}_{\overline{\mathbf{B}}}) \overline{\mathbf{B}} - w_2 \overline{\mathbf{B}}^2 = a \vec{e}_1 \otimes \vec{e}_1 + a_Q (\vec{e}_2 \otimes \vec{e}_2 + \vec{e}_3 \otimes \vec{e}_3)$$

and the abbreviations

$$\begin{aligned} a &= (w_1 + w_2 \mathbf{I}_{\overline{\mathbf{B}}}) \overline{B} - w_2 \overline{B}^2 \\ a_Q &= (w_1 + w_2 \mathbf{I}_{\overline{\mathbf{B}}}) \overline{B}_Q - w_2 \overline{B}_Q^2 \end{aligned}$$

to the deviator

$$\left(\frac{d\overline{v}}{d\overline{\mathbf{B}}} \overline{\mathbf{B}} \right)^D = b \vec{e}_1 \otimes \vec{e}_1 - \frac{b}{2} (\vec{e}_2 \otimes \vec{e}_2 + \vec{e}_3 \otimes \vec{e}_3) \quad (4.1)$$

with $b = 2/3 \left((w_1 + w_2 \mathbf{I}_{\overline{\mathbf{B}}}) (\overline{B} - \overline{B}_Q) - w_2 (\overline{B}^2 - \overline{B}_Q^2) \right)$. Here, strain-energies (2.26) with $K = 1000$ MPa, $\hat{\alpha} = 0.00367$ MPa, $c_{01} = 0.1958$ MPa and $c_{10} = 0.1788$ MPa are applied. Additionally, the first and second invariant of the unimodular left Cauchy-Green tensors have to be calculated

$$\begin{aligned} \mathbf{I}_{\overline{\mathbf{B}}} &= \mathbf{I}_{\overline{\mathbf{C}}} = \text{tr} \overline{\mathbf{B}} = \overline{B} + 2\overline{B}_Q = (\lambda \lambda_Q^2)^{-2/3} (\lambda^2 + 2\lambda_Q^2) \\ \mathbf{II}_{\overline{\mathbf{B}}} &= \mathbf{II}_{\overline{\mathbf{C}}} = \frac{1}{2} (\mathbf{I}_{\overline{\mathbf{B}}} - \text{tr} \overline{\mathbf{B}}^2) = \text{tr} (\overline{\mathbf{B}}^{-1}) = (\lambda \lambda_Q^2)^{2/3} (\lambda^{-2} + 2\lambda_Q^{-2}) \end{aligned} \quad (4.2)$$

From Eq. (2.42), expressed by the component representation of the Cauchy stress tensor and (4.1), the two equations

$$\begin{aligned}\sigma &= \frac{\rho_R \Theta}{\varphi \Theta_0} U'(J/\varphi) + \frac{4\rho_R \Theta}{3\lambda\lambda_Q^2 \Theta_0} \left((w_1 + w_2 \mathbf{I}_{\overline{\mathbf{B}}})(\overline{\mathbf{B}} - \overline{\mathbf{B}}_Q) - w_2(\overline{\mathbf{B}}^2 - \overline{\mathbf{B}}_Q^2) \right) \\ 0 &= \frac{\rho_R \Theta}{\varphi \Theta_0} U'(J/\varphi) - \frac{2\rho_R \Theta}{3\lambda\lambda_Q^2 \Theta_0} \left((w_1 + w_2 \mathbf{I}_{\overline{\mathbf{B}}})(\overline{\mathbf{B}} - \overline{\mathbf{B}}_Q) - w_2(\overline{\mathbf{B}}^2 - \overline{\mathbf{B}}_Q^2) \right)\end{aligned}\quad (4.3)$$

result. In other words, for a given axial stretch λ and temperature Θ , Eq. (4.3)₂ has to be iteratively solved to obtain the lateral stretch λ_Q . In the second step, the entire true stress, (4.4)₁, can be evaluated.

Obviously, the experimentally observed “linear” dependence of the temperature difference becomes obvious in a stress-stretch diagram, see Fig. 1. It has to be remarked, that the function $\hat{\varphi}(\vartheta)$ defined in Eq. (2.6) with $\alpha = 2.06 \cdot 10^{-4} \text{ K}^{-1}$ (see Heimes, 2005), has no essential influence in the range of applications, so that the behavior is close to linear behavior.

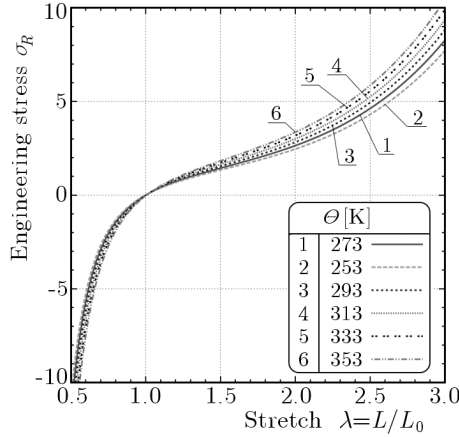


Fig. 1. Simple tension for constant temperatures ($\Theta_0 = 273 \text{ K}$). Representation of the linear temperature dependence. σ_R defines the 1st PK-stress component

As mentioned in Hartmann and Neff (2003), the strain-energy part $U(J_M) = K/2(J_M - 1)^2$, commonly applied in commercial finite element computations, yields in the case of uniaxial tensile tests an increase of the lateral stretch above a certain amount of the lateral stretch (i.e. the specimen becomes thicker in the tensile range). Vice versa, in compression, the specimen becomes thinner below a certain compressive stress state. Accordingly, the investigation of the sensitivity of $J_M = J/\hat{\varphi}(\vartheta)$ is of interest. In Fig. 2a the expected non-physical behavior is shown. Again, there is no essential influence

of the temperature-dependence introduced by $\hat{\varphi}(\vartheta)$. All curves are very close to each other. Proposal (2.26)₁ does not show such non-physical behavior, see Fig. 2b. Unfortunately, there does not exist an analytical proof guaranteeing this property. Only computations in a wide range of stretches and parameters indicate this behavior.

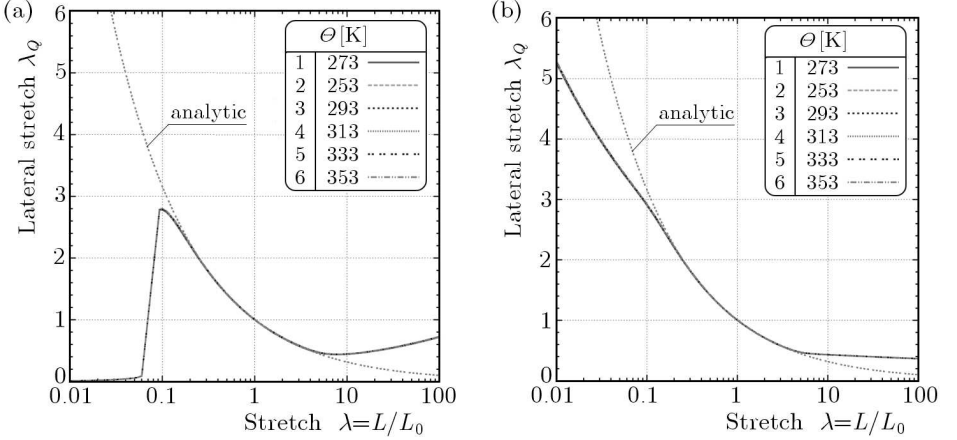


Fig. 2. Lateral stretches for various strain-energy functions $U(J_M) = U(J/\varphi)$ with $K = 1000$ MPa; (a) $U(J_M) = K/2(J_M - 1)^2$, (b) $U(J_M) = K/50(J_M^5 + J_M^{-5} - 2)$

4.2. Finite element computations

The proposed solution scheme using Rosenbrock-type methods is demonstrated at one-eighths of an elastomeric specimen shown in Fig. 3. The material parameters are those of the previous example, and for the thermal part we define $\kappa = 0.26$ W/mK and $\Theta_0 = 293.15$ K. Additionally, convection is assumed at the outer surfaces with $q(t) = h_0(\Theta - \Theta_\infty)$, $h_0 = 12.5$ W/m²K and $\Theta_\infty = 293.15$ K. Since the heat flux depends essentially on the surface deformation (spatial quantity), the numerical treatment of the deformation-dependent heat flux has to be taken into considerations (this is not discussed here). The mechanical and thermal boundary conditions are described in Fig. 3. One simplification is the negligence of the first term in Eq. (3.3), which is very small for $J \approx 1$. With the thermal part of free-energy (2.27), one obtains $c_p = c_{p0}(1 + k_p\Theta)$, where $c_{p0} = 1.54 \cdot 10^3$ J/kgK and $k_p = 3.75 \cdot 10^{-3}$ K⁻¹ are assumed (see Heimes, 2005).

In order to study the step-size behavior, the specimen is loaded sinusoidally with 200 cycles in the first 200 s. Afterwards, the displacements $\bar{u}_z(t) = -10$ mm, $t \geq 200$ s, are held constant, Fig. 4a. A step-size control-

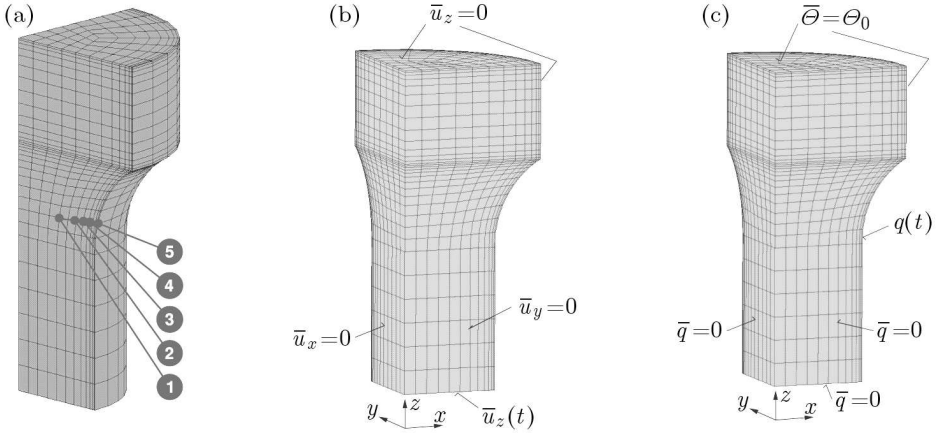


Fig. 3. Evaluations points, mechanical and thermal boundary conditions for a mesh using eight-noded Q1P0-elements; (a) evaluation points, (b) mechanical boundary conditions, (c) thermal boundary conditions, $q(t) = h_0(\Theta - \Theta_\infty)$

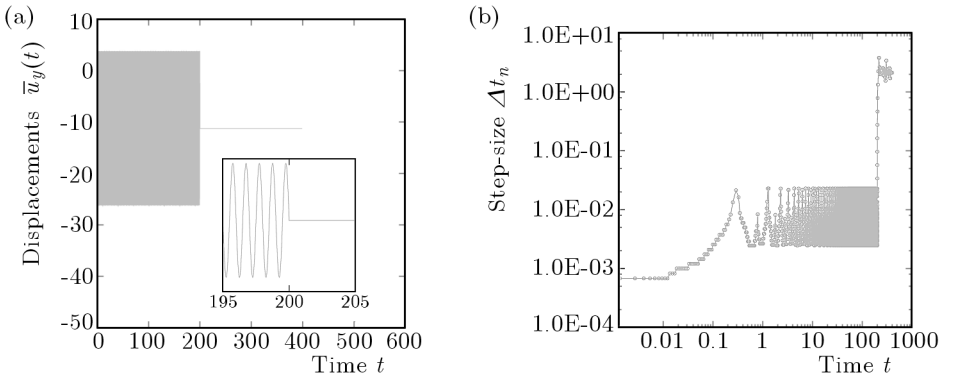


Fig. 4. Loading path and the resulting step-size behavior; (a) sine loading path with 200 cycles, (b) step-size behavior of the integration method

led third-order method of Rang and Angermann (2008) with an embedded method of order two to estimate the local error is applied to resolve the complicated temperature-deformation behavior. The temperature increases in a non-sinusoidal manner, see zoomed picture in Fig. 5b, which is a known fact (see Reese, 2001). Moreover, different time-scales (e.g. the final hold-time of 200 s) cannot be efficiently solved with constant step-sizes so that a step-size control technique is recommendable. Figure 5a shows the increase of the temperature in the specimen during cyclic loading which has the tendency to reach saturation caused by the influence of convection. During the hold-time $200 \leq t \leq 400$ s, the temperature decreases caused by convection as well.

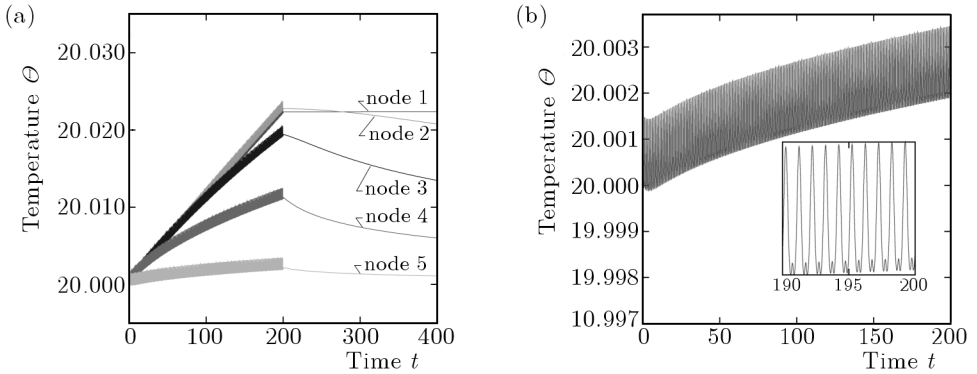


Fig. 5. Temperature evolution; (a) temperature evolution at marked nodes, see Fig. 3a, (b) temperature evolution at marked node 5

In Fig. 6 it is shown, at different times, that the heat evolution requires a good spatial resolution close to the surface, where a finer mesh is used.

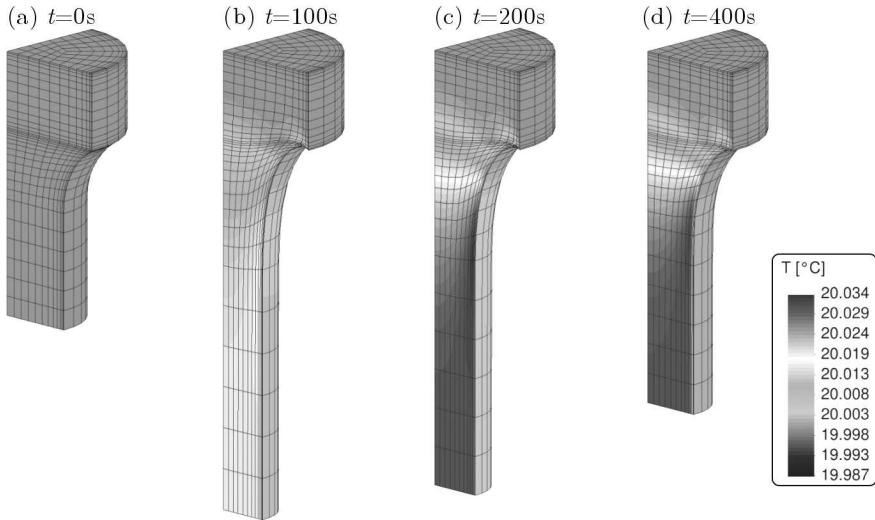


Fig. 6. Temperature evolution for time $t = 0, 100, 200, 400$ s

5. Conclusions

A consistent decomposition into thermal and mechanical as well as isochoric and volumetric effects is applied to the case of thermo-hyperelasticity. A particular poly-convex strain-energy function based on invariants of the uni-

modular Cauchy-Green tensors is extended to the thermo-mechanical case. Even in this case, it is demonstrated that a physical meaningful uniaxial tensile/compression case requires specific strain-energies. These models are incorporated in a fully thermo-mechanical coupled finite element program, where a totally iteration-free third-order Rosenbrock-type method to solve the coupled DAE-system given by the heat equation and equilibrium conditions offers a very efficient possibility to solve cyclic loading with different time-scales.

Acknowledgment

This paper is based on investigations of a grant given by the *Simulationswissenschaftliche Zentrum* of the Clausthal University of Technology. We would like to express our sincere thanks.

References

1. EHLERS W., EIPPER G., 1998, The simple tension problem at large volumetric strains computed from finite hyperelastic material laws, *Acta Mechanica*, **130**, 17-27
2. FLORY P.J., 1961, Thermodynamic relations for high elastic materials, *Transaction of the Faraday Society*, **57**, 829-838
3. GEAR C.W., 1986, Maintaining solution invariants in the numerical solution of ODEs, *SIAM Journal on Scientific and Statistical Computing*, **7**, 3, 734-743
4. HAIRER E., WANNER G., 1996, *Solving Ordinary Differential Equations II*, Springer, Berlin, 2nd revised edition
5. HARTMANN S., 2001a, Numerical studies on the identification of the material parameters of Rivlin's hyperelasticity using tension-torsion tests, *Acta Mechanica*, **148**, 129-155
6. HARTMANN S., 2001b, Parameter estimation of hyperelasticity relations of generalized polynomial-type with constraint conditions, *International Journal of Solids and Structures*, **38**, 44/45, 7999-8018
7. HARTMANN S., 2002, Computation in finite strain viscoelasticity: finite elements based on the interpretation as differential-algebraic equations, *Computer Methods in Applied Mechanics and Engineering*, **191**, 13/14, 1439-1470
8. HARTMANN S., HAMKAR A.-W., 2010, Rosenbrock-type methods applied to finite element computations within finite strain viscoelasticity, *Computer Methods in Applied Mechanics and Engineering*, **199**, 23/24, 1455-1470
9. HARTMANN S., NEFF P., 2003, Polyconvexity of generalized polynomial-type hyperelastic strain energy functions for near-incompressibility, *International Journal of Solids and Structures*, **40**, 11, 2767-2791

10. HARTMANN S., QUINT K.J., HAMKAR, A.-W., 2008, Displacement control in time-adaptive non-linear finite-element analysis, *Journal of Applied Mathematics and Mechanics*, **88**, 5, 342-364
11. HARTMANN S., WENSCH J., 2007, Finite element analysis of viscoelastic structures using Rosenbrock-type methods, *Computational Mechanics*, **40**, 383-398
12. HAUPT P., 1985, On the concept of an intermediate configuration and its application to representation of viscoelastic-plastic material behavior, *International Journal of Plasticity*, **1**, 303-316
13. HAUPT P., 2002, *Continuum Mechanics and Theory of Materials*, Springer, Berlin, 2 edition
14. HAUPT P., TSAKMAKIS C., 1989, On the application of dual variables in continuum mechanics, *Journal of Continuum Mechanics and Thermodynamics*, **1**, 165-196
15. HAUPT P., TSAKMAKIS C., 1996, Stress tensors associated with deformation tensors via duality, *Archive of Mechanics*, **48**, 347-384
16. HEIMES T., 2005, *Finite Thermoelastizität*, Number 709 in Fortschrittsberichte, Reihe 5, Grund- und Werkstoffe/Kunststoffe, VDI-Verlag, Düsseldorf
17. HOLZAPFEL G., SIMO J., 1996a, A new viscoelastic constitutive model for continuous media at finite thermomechanical changes, *International Journal of Solids and Structures*, **33**, 3019-3034
18. HOLZAPFEL G., SIMO J., 1996b, Entropy elasticity of isotropic rubber-like solids at finite strains, *Computer Methods in Applied Mechanics and Engineering*, **132**, 17-44
19. LANG J., 2000, *Adaptive multilevel solution of nonlinear parabolic PDE systems. Theory, algorithm, and applications*, Springer, Berlin
20. LION A., 1997, A physically based method to represent the thermomechanical behaviour of elastomers, *Acta Mechanica*, **123**, 1-26
21. LION A., 2000, *Thermomechanik von Elastomeren. Experimente und Materialtheorie*, Habilitation, Institute of Mechanics, University of Kassel, Report No. 1/2000
22. LU S., PISTER K., 1975, Decomposition of deformation and representation of the free energy function for isotropic thermoelastic solids, *International Journal of Solids and Structures*, **11**, 927-934
23. LUBICH C., ROCHE M., 1990, Rosenbrock methods for differential-algebraic systems with solution-dependent singular matrix multiplying the derivative, *Computing*, **43**, 325-342
24. MIEHE C., 1988, *Zur numerischen Behandlung thermomechanischer Prozesse*, Report No. F88/6, University of Hannover, Institut für Baumechanik und Numerische Mechanik
25. MIEHE C., 1995, Entropic thermoelasticity at finite strains. Aspects of the formulation and numerical implementation, *Computer Methods in Applied Mechanics and Engineering*, **120**, 243-269

26. RANG J., ANGERMANN L., 2008, New Rosenbrock methods of order 3 for PDAEs of index 2, *Advances in Differential Equations and Control Processes*, **1**, 2, 193-217
27. REESE S., 2001, *Thermomechanische Modellierung gummiartiger Polymer-Strukturen*, Habilitation, Institut für Baumechanik und Numerische Mechanik, Universität Hannover, Report No. F01/4
28. SIMO J.C., MIEHE C., 1992, Associative coupled thermoplasticity at finite strains: Formulation, numerical analysis and implementation, *Computer Methods in Applied Mechanics and Engineering*, **98**, 41-104
29. SIMO J.C., TAYLOR R.L., 1991, Quasi-incompressible finite elasticity in principal stretches. Continuum basis and numerical algorithms, *Computer Methods in Applied Mechanics and Engineering*, **85**, 273-310
30. SIMO J.C., TAYLOR R.L., PISTER K.S., 1985, Variational and projection methods for the volume constraint in finite deformation elasto-plasticity, *Computer Methods in Applied Mechanics and Engineering*, **51**, 177-208
31. TRELOAR L.R.G., 1975, *The Physics of Rubber Elasticity*, Clarendon Press, Oxford, 3rd edition

Teoretyczne i numeryczne aspekty słabo ściśliwego sformułowania termosprężystości dużych deformacji

Streszczenie

W pracy przedstawiono model niemal nieściśliwego, sprężystego zachowania się materiału, rozszerzając go na efekty termiczne. Na początku rozważań dokonano multiplikatywnej dekompozycji gradientu deformacji na część termiczną i mechaniczną. Część termiczna wykazuje charakter czysto objętościowy. Dodatkowo, część mechaniczną zdekomponowano na element zachowujący objętość i element o zmiennej objętości w ten sposób, że wypadkowy stan naprężeń wykazuje wrażliwość na temperaturę. Zaproponowany model szczegółowo zbadano w kontekście efektów sprzężenia termomechanicznego. W dalszej części pracy, analizowany model zastosowano do czasowo adaptacyjnej metody elementów skończonych sformułowanej na podstawie metod Rosenbrocka wyższych rzędów. Takie sformułowanie umożliwia uzyskanie procedury beziteracyjnej, co z kolei pozwala na wykonanie wyjątkowo szybkich obliczeń numerycznych. Artykuł zamyka przykład symulacji numerycznej trójwymiarowej próbki elastomeru poddanej próbie rozciągania.

Manuscript received December 1, 2010; accepted for print April 1, 2011